SUPER-RESOLUTION OF MULTISPECTRAL IMAGES

R. MOLINA[a*], J. MATEOS[a] and M. VEGA[b]

a) Dept. Ciencias de la Computación e I. A., Univ. de Granada,
b) Dept. de Lenguajes y Sistemas Informáticos, Univ. de Granada,
18071 Granada, Spain
**E-mail:rms@decsai.ugr.es*

A.K. KATSAGGELOS

Dept. of Electrical Engineering and Computer Science,
Northwestern University, Evanston, Illinois 60208-3118. USA

In this paper we analyze global and locally adaptive super resolution Bayesian methodology for pansharpening of multispectral images. The discussed methodologies incorporate prior knowledge on the expected characteristics of the multispectral images, uses the sensor characteristics to model the observation process of both panchromatic and multispectral images, and includes information on the unknown parameters in the model in the form of hyperprior distributions. Using real and synthetic data, the pansharpened multispectral images are compared with the images obtained by other parsharpening methods and their quality is assessed both qualitatively and quantitatively.

Keywords: Super-resolution; Bayesian Models; Hyperspectral Images.

1. Introduction

Nowadays most remote sensing systems include sensors able to simultaneously capture several low resolution images of the same area on different wavelengths, thus forming a multispectral image, along with a high resolution panchromatic image. The main characteristics of such remote sensing systems are the number of bands of the multispectral image and the resolution of those bands and the panchromatic image. The main advantage of the multispectral image is to allow for a better land type and use recognition but, due to its lower resolution, information on the objects' shape and texture may be lost. On the other hand, the panchromatic image allows for a better recognition of the objects in the image and their textures but provides no information about their spectral properties.

Throughout this paper the term *multispectral image reconstruction* will refer to the joint processing of the multispectral and panchromatic images

in order to obtain a new multispectral image that, ideally, will exhibit the spectral characteristics of the observed multispectral image and the resolution and quality of the panchromatic image.

A few approximations to multispectral image reconstruction have been proposed in the literature (see, for instance, Ref. 1–4) including a few super-resolution based methods.[5,6]

In this paper we follow the hierarchical Bayesian approach to obtain a solution to the super resolution reconstruction of multispectral images problem and discuss the utilization of global and spatially varying image models. Then, applying variational methods to approximate probability distributions, we estimate the unknown parameters, and the high resolution multispectral image.

The paper is organized as follows. In section 2 the Bayesian modeling and inference for super resolution reconstruction of multispectral images is presented. The required probability distributions for the Bayesian modeling of the super resolution problem are formulated in section 3. The Bayesian analysis and posterior probability approximation to obtain the parameters and the super resolution reconstructed image is performed in section 4. Experimental results on a real Landsat 7 ETM+ image are described in section 5 and, finally, section 6 concludes the paper.

2. Bayesian Problem Formulation

Let us assume that $\mathbf{y}$, the multispectral image we would observe under ideal conditions with a high resolution sensor, has B bands $\mathbf{y}_b$, $b = 1, \ldots, B$, that is, $\mathbf{y} = [\mathbf{y}_1^t, \mathbf{y}_2^t, \ldots, \mathbf{y}_B^t]^t$, where each band is of size $p = m \times n$ pixels and t denotes the transpose of a vector or matrix. Each band of this image is expressed above as a column vector by lexicographically ordering its pixels. In real applications, this high resolution image is not available. Instead, we observe a low resolution multispectral image $\mathbf{Y}$ with B bands $\mathbf{Y}_b$, $b = 1, \ldots, B$, that is, $\mathbf{Y} = [\mathbf{Y}_1^t, \mathbf{Y}_2^t, \ldots, \mathbf{Y}_B^t]^t$, where each band is of size $P = M \times N$ pixels with $M < m$ and $N < n$. Each band of this image is also expressed as a column vector by lexicographically ordering its pixels. The sensor also provides us with a panchromatic image $\mathbf{x}$ of size $p = m \times n$, obtained by spectrally averaging the unknown high resolution images $\mathbf{y}_b$.

The objective of the high resolution multispectral image reconstruction problem is to obtain an estimate of the unknown high resolution multispectral image $\mathbf{y}$ given the panchromatic high resolution observation $\mathbf{x}$ and the low resolution multispectral observation $\mathbf{Y}$.

Using the hierarchical Bayesian paradigm (see, for example, Ref. 7) the

following joint distribution for $\mathbf{\Omega}_M$, $\mathbf{y}$, $\mathbf{Y}$, and $\mathbf{x}$ is defined $\mathrm{p}(\mathbf{\Omega}_M, \mathbf{y}, \mathbf{Y}, \mathbf{x}) = \mathrm{p}(\mathbf{\Omega}_M)\mathrm{p}(\mathbf{y}|\mathbf{\Omega}_M)\mathrm{p}(\mathbf{Y}, \mathbf{x}|\mathbf{y}, \mathbf{\Omega}_M)$, where $\mathbf{\Omega}_M$ denotes the set of hyperparameters needed to describe the required probability density functions (obvioulsy, depending on the set of hyperparameters the probability models used in the problem will differ).

The Bayesian paradigm dictates that inference on the unknowns $(\mathbf{\Omega}_M, \mathbf{y})$, should be based on $\mathrm{p}(\mathbf{\Omega}_M, \mathbf{y}|\mathbf{Y}, \mathbf{x}) = \mathrm{p}(\mathbf{\Omega}_M, \mathbf{y}, \mathbf{Y}, \mathbf{x})/\mathrm{p}(\mathbf{Y}, \mathbf{x})$.

3. Bayesian Modeling

We assume that $\mathbf{Y}$ and $\mathbf{x}$, for a given $\mathbf{y}$ and a set of parameters $\mathbf{\Omega}_M$, are independent and consequently write $\mathrm{p}(\mathbf{Y}, \mathbf{x}|\mathbf{y}, \mathbf{\Omega}_M) = \mathrm{p}(\mathbf{Y}|\mathbf{y}, \mathbf{\Omega}_M)\mathrm{p}(\mathbf{x}|\mathbf{y}, \mathbf{\Omega}_M)$.

Each band, $\mathbf{Y}_b$, is related to its corresponding high resolution image by

$$\mathbf{Y}_b = \mathbf{D}\mathbf{H}\mathbf{y}_b + \mathbf{n}_b, \quad \forall b = 1, \cdots, B, \tag{1}$$

where $\mathbf{H}$ is a $p \times p$ blurring matrix and $\mathbf{D}$ is a $P \times p$ decimation operator and $\mathbf{n}_b$ is the capture noise, assumed to be Gaussian with zero mean and variance $1/\beta_b$.

Given the degradation model for multispectral image super-resolution described by Eq. (1) and assuming independence between the noise observed in the low resolution images, the distribution of the observed $\mathbf{Y}$ given $\mathbf{y}$ and a set of parameters $\mathbf{\Omega}_M$ is

$$\mathrm{p}(\mathbf{Y}|\mathbf{y}, \mathbf{\Omega}_M) = \prod_{b=1}^{B} \mathrm{p}(\mathbf{Y}_b|\mathbf{y}_b, \beta_b) \propto \prod_{b=1}^{B} {\beta_b}^{P/2} \exp\left\{-\frac{1}{2}\beta_b \parallel \mathbf{Y}_b - \mathbf{H}\mathbf{y}_b \parallel^2\right\}. \tag{2}$$

As already described, the panchromatic image $\mathbf{x}$ is obtained by spectrally averaging the unknown high resolution images $\mathbf{y}_b$, modeled as

$$\mathbf{x} = \sum_{b=1}^{B} \lambda_b \mathbf{y}_b + \mathbf{v}, \tag{3}$$

where $\lambda_b \geq 0$, $b = 1, 2, \cdots, B$, are known quantities that can be obtained, as we will see later, from the sensor spectral characteristics, and $\mathbf{v}$ is the capture noise that is assumed to be Gaussian with zero mean and variance γ^{-1}. Note that, usually, $\mathbf{x}$ does not depend on all the multispectral image bands but on a subset of them, i. e., some of the λ_b's are equal to zero.

Using the degradation model in Eq. (3), the distribution of the panchromatic image $\mathbf{x}$ given $\mathbf{y}$, and a set of parameters $\mathbf{\Omega}$ is given by

$$\mathrm{p}(\mathbf{x}|\mathbf{y}, \mathbf{\Omega}_M) \propto \gamma^{p/2} \exp\left\{-\frac{1}{2}\gamma \parallel \mathbf{x} - \sum_{b=1}^{B} \lambda_b \mathbf{y}_b \parallel^2\right\}. \tag{4}$$

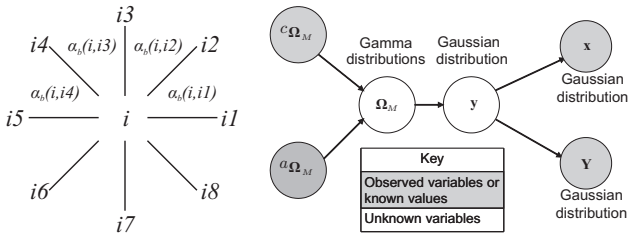

Fig. 1. (a) Pixel and inverse variance notation. (b) Graphical model showing the relationships between the variables.

From the above definition the parameter vector $(\gamma, \beta_1, \ldots, \beta_B)$ is a subset of $\mathbf{\Omega}_M$. However, although the estimation of $(\gamma, \beta_1, \ldots, \beta_B)$ can be easily incorporated into the estimation process, we will assume here that these parameters have been estimated in advance and concentrate on gaining insight into the distribution of the prior image parameters, as described next.

3.1. *Global and Local Image Modeling*

In this paper we do not use the correlation among different high resolution bands but concentrate instead on modeling the local variation at each band.

In our global image model we assume a Conditional Auto-Regressive (CAR) model.[8] Then we have for the global model $M = G$,

$$\mathrm{p}_G(\mathbf{y}|\mathbf{\Omega}_G) \propto \prod_{b=1}^{B} \bar{\alpha}_b^{\frac{p}{2}} \exp\left\{-\frac{1}{2}\bar{\alpha}_b \left[\mathbf{y}_b^t \mathbf{C} \mathbf{y}_b\right]\right\}, \tag{5}$$

where $\mathbf{C}$ is the laplacian operator. The set of hyperparameters then becomes $\mathbf{\Omega}_G = (\bar{\alpha}_1, \ldots, \bar{\alpha}_B)$.

We now proceed to define a local model $M = L$, for the high resolution multispectral image. In its definition we use the notation $i1, i2, \ldots, i8$ to denote the eight pixels around pixel i (see Fig. 1(a)). Then following the approximation in Ref. 9 which extends Conditional Auto-Regressions to take into account local variability we write (see Ref. 10)

$$\mathrm{p}(\mathbf{y}|\mathbf{\Omega}_L) = \prod_{b=1}^{B} \mathrm{p}(\mathbf{y}_b|\boldsymbol{\alpha}_b) \propto \prod_{b=1}^{B}\prod_{i=1}^{p}\prod_{l=1}^{4} \alpha_b(i,il)^{\frac{1}{8}} \exp\left\{-\frac{1}{2}\alpha_b(i,il)[y_b(i) - y_b(il)]^2\right\}, \tag{6}$$

where $\alpha_b(i, il)$ controls, for the b-band, the smoothness of the restoration between pixels i and il and $\boldsymbol{\alpha}_b = (\alpha_b(i, il) \mid i = 1, \ldots, p,\ l = 1, \ldots, 4)$.

The set of hyperparameters then becomes $\mathbf{\Omega}_L = (\boldsymbol{\alpha}_1, \ldots, \boldsymbol{\alpha}_B)$. Note that if $\alpha_b(i, il) = \bar{\alpha}_b$, $i = 1, \ldots, p$, $l = 1, \ldots, 4$, the local image model becomes the global model defined above.

A large part of the Bayesian literature is devoted to finding hyperprior distributions $\mathrm{p}(\mathbf{\Omega}_M),\ M \in \{G, L\}$, for which $\mathrm{p}(\mathbf{\Omega}_M, \mathbf{y}|\mathbf{x}, \mathbf{Y})$ can be calculated in a straightforward way or can be approximated. These are the so called conjugate priors that, as we will see later, have the intuitive feature of allowing one to begin with a certain functional form for the prior and end up with a posterior of the same functional form, but with the parameters updated by the sample information.

Taking the above considerations about conjugate priors into account, we will assume for the hyperparameters of the global model that

$$\mathrm{p}(\mathbf{\Omega}_G) = \prod_{b=1}^{B} \mathrm{p}(\bar{\alpha}_b \mid \bar{a}_b^o, \bar{c}_b^o), \tag{7}$$

$\bar{c}_b^o > 0$ and $\bar{a}_b^o > 0$, while for the local model we will use the following distribution on the hyperparameters

$$\mathrm{p}(\mathbf{\Omega}_L) = \prod_{b=1}^{B} \prod_{i=1}^{p} \prod_{l=1}^{4} \mathrm{p}(\alpha_b(i, il) \mid a_b^o, c_b^o), \tag{8}$$

where $c_b^o > 0$ and $a_b^o > 0$ (note that the same hyperprior is assumed for all the α's in the same band).

In both, the local and global models, gamma distributions are used to define the hyperpriors of the precision parameters αs, that is, for $\omega \in \mathbf{\Omega}_M$ we have

$$\mathrm{p}(\omega \mid u_\omega, v_\omega) \propto \omega^{u_\omega - 1} \exp[-v_\omega \omega], \tag{9}$$

where $u_\omega > 0$ and $v_\omega > 0$. This gamma distribution has the following mean and variance

$$\mathbf{E}[\omega] = u_\omega / v_\omega, \qquad \mathbf{var}[\omega] = u_\omega / v_\omega^2. \tag{10}$$

Finally, combining the first and second stage of the problem modeling we have the global distribution

$$\mathrm{p}(\mathbf{\Omega}_M, \mathbf{y}, \mathbf{Y}, \mathbf{x}) = \mathrm{p}(\mathbf{\Omega}_M)\mathrm{p}(\mathbf{y}|\mathbf{\Omega}_M)\mathrm{p}(\mathbf{Y}|\mathbf{y})\mathrm{p}(\mathbf{x}|\mathbf{y}), \tag{11}$$

for $M \in \{G, L\}$. The joint probability model is shown in Fig. 1(b).

4. Bayesian inference and variational approximation of the posterior distribution for super resolution reconstruction of multispectral images

For our selection of hyperparameters in the previous section, the set of all unknowns is $(\mathbf{\Omega}_M, \mathbf{y})$.

As already explained, the Bayesian paradigm dictates that inference on $(\mathbf{\Omega}_M, \mathbf{y})$ should be based on $\mathrm{p}(\mathbf{\Omega}_M, \mathbf{y}|\mathbf{Y}, \mathbf{x})$. Since $\mathrm{p}(\mathbf{\Omega}_M, \mathbf{y}|\mathbf{Y}, \mathbf{x})$ can not be found in closed form, we will apply variational methods to approximate this distribution by the distribution $\mathrm{q}(\mathbf{\Omega}_M, \mathbf{y})$.

The variational criterion used to find $\mathrm{q}(\Omega_M, \mathbf{y})$ is the minimization of the Kullback-Leibler divergence, given by[11,12]

$$C_{KL}(\mathrm{q}(\mathbf{\Omega}_M, \mathbf{y})||\mathrm{p}(\mathbf{\Omega}_M, \mathbf{y}|\mathbf{Y}, \mathbf{x})) = \int \mathrm{q}(\mathbf{\Omega}_M, \mathbf{y}) \log\left(\frac{\mathrm{q}(\mathbf{\Omega}_M, \mathbf{y})}{\mathrm{p}(\mathbf{\Omega}_M, \mathbf{y}|\mathbf{Y}, \mathbf{x})}\right) d\Omega_M d\mathbf{y}$$

$$= \int \mathrm{q}(\mathbf{\Omega}_M, \mathbf{y}) \log\left(\frac{\mathrm{q}(\mathbf{\Omega}_M, \mathbf{y})}{\mathrm{p}(\mathbf{\Omega}_M, \mathbf{y}, \mathbf{Y}, \mathbf{x})}\right) d\mathbf{\Omega}_M d\mathbf{y} + \text{const}, \tag{12}$$

which is always non negative and equal to zero only when $\mathrm{q}(\mathbf{\Omega}_M, \mathbf{y}) = \mathrm{p}(\mathbf{\Omega}_M, \mathbf{y}|\mathbf{Y}, \mathbf{x})$.

We choose to approximate the posterior distribution $\mathrm{p}(\mathbf{\Omega}_M, \mathbf{y}|\mathbf{Y}, \mathbf{x})$ by the distribution

$$\mathrm{q}(\mathbf{\Omega}_M, \mathbf{y}) = \mathrm{q}(\mathbf{\Omega}_M)\mathrm{q}_D(\mathbf{y}), \tag{13}$$

where $\mathrm{q}(\mathbf{\Omega}_M)$ denotes a distribution on $\mathbf{\Omega}_M$ and $\mathrm{q}_D(\mathbf{y})$ denotes a degenerate distribution on $\mathbf{y}$.

Note that other distribution approximations are also possible. However, as we will see later the one used here alleviates the problem of having to estimate an enormous amount of hyperparameters. We now proceed to find the best of these distributions in the divergence sense. Let us assume that $\mathbf{y}^k$ is the current estimate of the multispectral image where $\mathrm{q}_D(\mathbf{y})$ is degenerate.

Given $\mathrm{q}_D^k(\mathbf{y})$, we can obtain an estimate of $\mathrm{q}(\mathbf{\Omega})$ which reduces the KL-divergence by solving

$$\mathrm{q}^{k+1}(\mathbf{\Omega}_M) = \arg \min_{\mathrm{q}(\mathbf{\Omega}_M)} C_{KL}(\mathrm{q}(\mathbf{\Omega}_M), \mathrm{q}_D^k(\mathbf{y}) \parallel \mathrm{p}(\mathbf{\Omega}_M, \mathbf{y}|\mathbf{Y}, \mathbf{x})). \tag{14}$$

Differentiating the integral in the right hand side of Eq. (14) with respect to $\mathrm{q}(\mathbf{\Omega}_M)$ and setting it equal to zero we have that if $M = G$ then $\mathrm{q}^{k+1}(\mathbf{\Omega}_G)$ satisfies $\mathrm{q}^{k+1}(\mathbf{\Omega}_G) = \prod_{b=1}^{B} \mathrm{q}^{k+1}(\bar{\alpha}_b)$, where $\mathrm{q}^{k+1}(\bar{\alpha}_b) = \mathrm{p}\left(\bar{\alpha}_b|\bar{a}_b^o + \frac{p}{2}, \bar{c}_b^o + \frac{1}{2}\left[\mathbf{y}_b^{k\,t}\mathbf{C}\mathbf{y}_b^k\right]\right)$. These distributions have the following means

$$\mathbf{E}[\bar{\alpha}_b]_{q^{k+1}(\mathbf{\Omega}_G)} = \frac{\bar{a}_b^o + \frac{p}{2}}{\bar{c}_b^o + \frac{1}{2}\left[\mathbf{y}_b^{k\,t}\mathbf{C}\mathbf{y}_b^k\right]}, \quad b = 1, \ldots, B, \tag{15}$$

which can be rewritten as

$$\frac{1}{\mathbf{E}[\bar{\alpha}_b]_{q^{k+1}(\mathbf{\Omega}_G)}} = \bar{\mu}_b \frac{\bar{c}_b^o}{\bar{a}_b^o} + (1 - \bar{\mu}_b)\frac{\mathbf{y}_b^{k\,t}\mathbf{C}\mathbf{y}_b^k}{p}, \quad b = 1, \ldots, B, \tag{16}$$

where $\bar{\mu}_b = \frac{\bar{a}_b^o}{p/2+\bar{a}_b^o}, \quad b = 1 \ldots, B.$

The above equations indicate that $\bar{\mu}_b$, $b = 1, \ldots, B$, can be understood as normalized confidence parameters taking values in the interval $[0, 1)$. That is, when they are zero no confidence is placed on the given hyperparameters, while when the corresponding normalized confidence parameter is asymptotically equal to one it fully enforces the prior knowledge of the mean (no estimation of the hyperparameters is performed). Furthermore, for each hyperparameter, the inverse of the mean of its posterior distribution approximation is a weighted sum of the inverse of the mean of its hyperprior distribution (see Eq. (10)) and its maximum likelihood estimate.

If we use the local image model, that is, $M = L$, we have

$$\mathrm{q}^{k+1}(\mathbf{\Omega}_L) = \prod_{b=1}^{B} \prod_{i=1}^{p} \prod_{l=1}^{4} \mathrm{q}^{k+1}(\alpha_b(i, il)),$$

where $\mathrm{q}^{k+1}(\alpha_b(i, il)) = \mathrm{p}\left(\alpha_b(i, il) \mid a_b^o + \frac{1}{8}, \frac{1}{2}[y_b^k(i) - y_b^k(il)]^2 + c_b^o\right)$. These distributions have the following means

$$\mathbf{E}[\alpha_b(i, il)]_{q^{k+1}(\mathbf{\Omega}_L)} = \frac{a_b^o + \frac{1}{8}}{c_b^o + \frac{1}{2}[y_b^k(i) - y_b^k(il)]^2} = \alpha_b^{k+1}(i, il). \tag{17}$$

Note that Eq. (17) can be rewritten as

$$\frac{1}{\mathbf{E}[\alpha_b(i, il)]_{q^{k+1}(\mathbf{\Omega}_L)}} = \mu_b \frac{c_b^o}{a_b^o} + (1 - \mu_b) 4[y_b^k(i) - y_b^k(il)]^2, \tag{18}$$

where $\mu_b = \frac{a_b^o}{a_b^o + \frac{1}{8}}$. These equations indicate, as for the global model, that μ_b can be understood as a normalized confidence parameter taking values in the interval $[0, 1)$.

Given now $\mathrm{q}^{k+1}(\mathbf{\Omega}_M)$ we can obtain an estimate of $\mathbf{y}_M^{k+1}$ (the value where $\mathrm{q}_D^{k+1}(\mathbf{y})$ is degenerate, which obviously will depend on the image model used) which reduces the KL-divergence by solving

$$\mathbf{y}_M^{k+1} = \arg\min_{\mathbf{y}} \left\{ -\mathbf{E}[\log \mathrm{p}(\mathbf{\Omega}_M, \mathbf{y}, \mathbf{Y}, \mathbf{x})]_{\mathrm{q}^{k+1}(\mathbf{\Omega}_M)} \right\}.$$

The convergence of the parameters defining the distributions $\mathrm{q}^{k+1}(\mathbf{\Omega}_M)$ and $\mathbf{y}_M^{k+1}$ can be used as stopping criterion for the iterative procedure that alternates between the estimation of both distributions.

5. Experimental Results

Let us now compare the use of the described local and global image models in the reconstruction of synthetic color images and real Landsat ETM+ images.

Fig. 2. (a) Original HR color image; (b) Observed LR color image (the image has been resized by zero-order hold to the size of the high resolution image for displaying purposes); (c) Panchromatic HR image; (d) Bicubic interpolation of (b); (e) Reconstruction using the global image model proposed in Ref. 8; (f) Reconstruction using the local image model proposed in Ref. 10.

Following Eq. (2), the color image in Fig. 2(a) was convolved with the mask $0.25 \times \mathbf{1}_{2\times 2}$ to simulate the sensor integration and then downsampled by a factor of two in each direction. Zero mean Gaussian noise with variance 4 was then added to obtain the observed LR image in Fig. 2(b). The panchromatic image, depicted in Fig. 2(c) was obtained from the original HR color image using the model in Eq. (3) with $\lambda_b = 1/3$, for $b = 1, 2, 3$, and Gaussian noise with variance 6.25.

The reconstruction provided by the global model proposed in Ref. 8 is shown in Fig. 2(e). The method in Ref. 8 was also used to estimate the parameters, β_b, $b = 1, 2, 3$, and γ. This method also provides values for the parameters $\bar{\alpha}_b$, $b = 1, 2, 3$ of the global image model. Several local model reconstructions were then obtained using the method in Ref. 10, they correspond to using as u_b^o/c_b^o values ranging from 10^{-2} to 10^2 times $\bar{\alpha}_b$ and in Eq. (18) values of μ_b ranging from 0 to 1 (note that knowing u_b^o/c_b^o and μ_b, the values of u_b^o and c_b^o can be calculated easily).

The spatial improvement of the reconstructed image has been assessed by means of the correlation of the high frequency components (COR) which

Table 1. PSNR and COR values for the color image reconstructions.

	PSNR			COR		
Band	1	2	3	1	2	3
Bicubic interpolation	12.7	12.7	12.7	0.50	0.50	0.51
Using the global image model	13.5	13.4	13.4	0.68	0.68	0.68
Using the local image model	18.9	19.0	18.9	0.99	0.99	0.99

measures the spatial similarity between each reconstructed multispectral image band and the panchromatic image, and spectral fidelity by means of the peak signal-to-noise ratio (PSNR) between the reconstructed and original multispectral image bands. Bicubic interpolation of each band was used as a reference method for comparison.

Table 1 depicts the resulting PSNR and COR values for all the reconstructed images. The table clearly shows that the proposed methods performs better than bicubic interpolation and that using a local image model provides considerably better results than using a global image one. Visual inspection of the results shows that with the use of a global image model we obtain improved spatial resolution but the details in the image are still oversmoothed. Using the local image model, however, we are able to incorporate the high frequency information from the panchromatic image into the reconstruction while preserving the spectral properties of the multispectral image.

Global and local image models are also compared on a real Landsat ETM+ image. Figure 3(a) depicts a 64×64 pixels false RGB color region of interest composed of bands 4, 3, and 2 of the Landsat ETM+ multispectral image, and Fig. 3(b) its corresponding 128×128 panchromatic image. The multispectral image was resized to the size of the panchromatic image for displaying purposes. The contribution of each multispectral image band to the panchromatic, that is, the values of λ_b, $b = 1, 2, \ldots, 4$, were calculated from the spectral response of the ETM+ sensor. The obtained values were equal to $0.0078, 0.2420, 0.2239$, and 0.5263, respectively. Reconstructions using the global and local image models are shown in Fig. 3(c) and 3(d), respectively. From these results it is clear that the local image model based method preserves the spectral properties of the multispectral image while successfully incorporating the high frequencies from the panchromatic image.

6. Conclusions

In this paper the reconstruction of multispectral images has been formulated from a superresolution point of view. A hierarchical Bayesian frame-

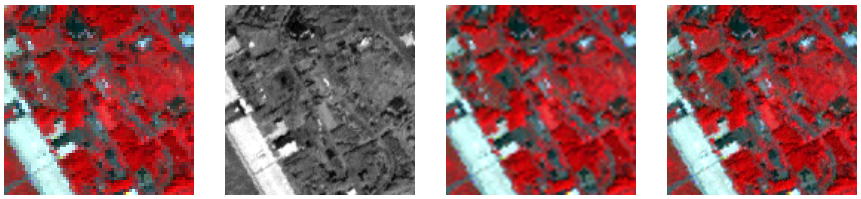

(a) (b) (c) (d)

Fig. 3. (a) Observed multispectral image; (b) Panchromatic image; (c) Reconstruction using the global image model; (d) Reconstruction using the local image model.

work has been presented to incorporate global and local prior knowledge on the expected characteristics of the multispectral images, model the observation process of both panchromatic and low resolution multispectral images, and also include information on the unknown parameters in the model in the form of hyperprior distributions. The methods have been tested experimentally.

References

1. W. J. Carper, T. M. Lillesand and R. W. Kiefer, *Phot. Eng. & Rem. Sens.* **56**, 459 (1990).
2. J. Nuñez, X. Otazu, O. Fors, A. Prades, V. Pala and R. Arbiol, *IEEE Trans on Geosc. & Rem. Sens.* **37**, 1204 (1999).
3. V. Vijayaraj, A quantitative analysis of pansharpened images, Master's thesis, Mississippi St. Univ. (2004).
4. J. Price, *IEEE Trans. on Geosc. & Rem. Sens.* **37**, 1199 (1999).
5. M. Eismann and R. Hardie, *IEEE Trans. on Geosc. & Rem. Sens.* **43**, 455 (2005).
6. T. Akgun, Y. Altunbasak and R. Mersereau, *IEEE Trans. on Img. Proc.* **14**, 1860 (2005).
7. R. Molina, A. K. Katsaggelos and J. Mateos, *IEEE Trans. on Img. Proc.* **8**, 231 (1999).
8. R. Molina, M. Vega, J. Mateos and A. Katsaggelos, *Applied and Computational Harmonic Analysis (accepted for publication)* (2007).
9. J. Chandas, N. P. Galatsanos and A. Likas, *IEEE Trans. on Image Processing* **15**, 2987 (2006).
10. R. Molina, J. Mateos and A. Katsaggelos, Super resolution of multispectral images using locally adaptive models, in *2007 European Sig. Proc. Conf. (EUSIPCO 2007), submitted*, 2007.
11. S. Kullback and R. A. Leibler, *Annals of Math. Stat.* **22**, 79 (1951).
12. S. Kullback, *Information Theory and Statistics* (Dover Publications, 1959).